Role of the porous structure of the bioceramic scaffolds in bone tissue engineering

Zhen Wang[1, 4], Jiang Chang[2, 4], Feng Bai[1, 4], Xiaojiang Sun[3], Kaili Lin[2], Lei Chen[2], Jianxi Lu[2]，Kerong Dai[3]

[1]Institute of Orthopedic Surgery, Xijing Hospital, Fourth Military Medical University, Xi'an 710032, P.R. China

[2]Shanghai Institute of Ceramics, Chinese Academy of Sciences, Shanghai 200050, P.R. China

[3]Department of Orthopaedic, Ninth People's Hospital, Shanghai JiaoTong University School of Medicine, 639 Zhizaoju Road, Shanghai 200011, People's Republic of China

[4]These authors contributed equally to this work.

Correspondence should be addressed to Kerong Dai (E-mail address: krdai@sibs.ac.cn) and Jianxi Lu (E-mail address :jianxilu@126.com).

The porous structure of biomaterials plays a critical role in improving the efficiency of biomaterials in tissue engineering. Here we fabricate successfully porous bioceramics with accurately controlled pore parameters, and investigate the effect of pore parameters on the mechanical property, the cell seeding proliferation and the vascularization of the scaffolds. This study shows that the porosity play an important role on the mechanical property of the scaffolds, which is affected not only by the macropores size, but also by the interconnections of the scaffolds. Larger pores are beneficial for cell growth in scaffolds. In contrast, the interconnections do not affect cell growth much. The interconnections appear to limit the number of blood vessels penatrating through adjacent pores, and both the pores size and interconnections can determine the size of blood vessels. The results may be referenced on the selective design of porous structure of biomaterials to meet the specificity of biological application.

Tissue engineering is a fast developing field, which focuses on the reconstruction and regeneration of defected and disfunctional tissues. The main bone tissue engineering approach is to seed living cells into porous materials to construct living tissues. Therefore, the physical-chemical and biological properties of the porous materials play a key role in the tissue reconstruction and regeneration process. Previous studies have shown that the porous structure of materials plays a critical role in determining the properties of the porous scaffolds, since it may directly or indirectly affect the mechanical and biological properties of the scaffolds[1-20]. For example, studies have shown that pore size of the porous bioceramics will affect vascularization and bone tissue in-growth as bone filling implants [1-12]. Other studies showed that cell metabolisms could be affected with different porosity [1-4]. However, the requirement

for materials as tissue engineering scaffolds is different as compared with that for the traditional implant materials. For tissue engineering applications, specific requirements for the mechanical manipulation, the cell seeding and infiltration, the vascularization of the scaffolds are critical, and the pore size, in particular, the size of the interconnections of the pores in tissue engineering scaffolds may be of great importance for tissue reconstruction.

To investigate the effect of the pore parameters on the properties of the tissue engineering materials, an accurate control of the pore size and the size of the interconnection is required and this is a big challenge in the fabrication of the porous bioceramics. In the present study, we used a template based technique to fabricate macroporous bioceramic scaffolds with accurately controlled pore parameters by using assembled microspheres as templates combined with casting technique. Under the accurate control of the pore parameters, the mechanical property, the cell seeding proliferation and metabolism in the scaffolds and the vascularization of the scaffolds were investigated.

RESULTS

Structural and mechanical properties of the porous ceramic scaffolds

For porous scaffold preparation, porous templates were first prepared by sticking the plastic macrospheres (300-700μm in diameter) together, and the contact between the macrospheres can be well controlled by controlling the preparation pressure and sticking time, which accurately determined the size of the interconnection of the ceramic scaffolds after sintering [21]. After preparation of the templates, ceramic slurry was prepared and cast into the template and ceramic scaffolds were obtained after sintering at 1100^{o}C (**Fig. 1**). Using this technique, we successfully fabricated ceramic scaffolds with accurately controlled pore size and interconnections (**Fig. 2** and **Table 1**).

In the present study, the relationship between the macrostructure and the mechanical properties of porous scaffolds was investigated. For the scaffolds with same interconnection and different pore size, an increase of the pore size resulted a decrease of the porosity and an increase of the compressive strength. For the scaffolds with same pore size and different interconnections, an increase of the interconnection resulted an increase of the porosity and a decrease of the compressive strength (**Fig. 3**).

Cell growth within the scaffolds

Using the ceramic scaffolds with different pore size and interconnections, cell seeding properties of these scaffolds were evaluated with bone marrow mesenchymal stem cells. The results showed that the number of seeded cells decreased with the increase of the size of macropores (from 300-400 to 600-700μm in diameter) and the constant interconnection size; while in scaffolds with constant size of macropores (300-400μm in diameter) only that with interconnection of 150μm showed less seeded cells than the scaffolds with other interconnection sizes in smaller diameters, and there were no statistical difference of the cell numbers between other

scaffolds*(P>0.05)* (**Fig. 4**).

Cell growth within the porous scaffolds is critical for the tissue reconstruction. Therefore, the cell proliferation in the scaffolds with different pore size (300-400, 400-500, 500-600 and 600-700μm in diameter)and interconnections(70, 100, 120, 150 and 200μm in diameter) was evaluated. The sample with 500-600μm pore size and constant interconnection of 120μm showed the highest cell proliferation with (**Fig.5a**), but there is no significant difference in cell proliferation with different interconnection and constant pore size of 300-400μm *(P>0.05)*(**Fig. 5b**)

Vascularization

Vascularization is one of the most important stages in the tissue regeneration and reconstruction of the living tissue. This study showed that the relationship between structural characteristics of the scaffolds such as the size of the pores and interconnections and the number and diameter of the blood vessels formed within the porous macrostructures of the scaffolds were closely correlated. The size of the blood vessel increased with the increase of the size of the interconnections($P<0.001$) (**Fig.6a-e**), while the increase of the pore size with constant interconnections did not affect the size of the blood vessels when the diameter of pores is larger than 400μm($P>0.05$) (**Fig.7c-e**). However, when the diameter of pores is smaller than 400μm, the size of the blood vessel decreased dramatically($P<0.001$) (**Fig.7a, b and e**). This result suggests that large pore size is beneficial for the growth of blood vessels, and the diameter of pore smaller than 400μm limits the growth of blood vessels and resulted in a smaller blood vessel diameter. In addition, it is clear to see that blood vessels grow fast within the porous scaffolds in the first 2 weeks, and then become stabilized, suggesting that the first 2 weeks are critical for development of the size of the blood vessels.

Similar to the effect on blood vessel size, the increase of the size of the interconnections also resulted in an increase of the number of the blood vessels ($P<0.001$) (**Fig.6a-d and f**), while the increase of the pore size with constant interconnections did not affect the number of the blood vessels formed within the macroporous structure as much as the interconnections. No significant difference in the number of the blood vessels was observed between the samples with different pore size and constant size of interconnections ($P=0.102$) (**Fig.7a-d and f**). It is also noticed that the number of blood vessels increased within the first 4 weeks in all samples and then become stabilized, suggesting that the number of the blood vessels was determined by the size of the interconnections in the first 4 weeks after implantation.

DISCUSSION

Mechanical property is critical for tissue engineering scaffolds, since one of the important roles of the scaffolds is to provide mechanical support for cells and tissues infiltrated and grew into the macrostructure of the scaffolds. It is a common knowledge that the mechanical strength decreases with the increase of the porosity.

However, no report has been found to show the relationship between the porosity and the interconnection of the porous scaffolds. One of our interesting results is that the porosity is also affected by the size of the interconnection. An increase of the size of the interconnection resulted in a decrease of the compressive strength, since the increase of the interconnection with constant pore size results in an increase of the porosity. This study confirmed that the porosity play an important role on the mechanical property of the scaffolds, which is affected not only by the size of the macropores, but also affected by the size of the interconnection of the scaffolds.

Generally speaking, the first step of the tissue engineering approach is to add cells into porous scaffolds. Therefore, it is important to investigate the relationship between pore parameters and cell seedings. Previous studies have shown that pore sizes and porosities have an effect on cell proliferation[1-12]. However, the results are controversy, since the shape of the pores and the interconnections between the pores are not uniform in most cases[1]. In our study, with the accurate control of the size of the pores and interconnections, the cell infiltration and growth could be reasonably evaluated. The results showed that both the pore size and the size of interconnections affected cell seeding and growth. When the interconnection was fixed at 120μm, the pores with a size of 300-400μm were the best for cell attachment and showed more cells in the scaffolds, and the larger pores resulted in a decrease of the cell numbers in the scaffolds. This result indicates that if the pores are larger than 400μm, some of the cells cannot be caught in the scaffolds during the seeding, so 300-400μm might be the best pore size for cell seeding. When the pore size is fixed at 300-400μm, 120μm seems to be the up limit size of the interconnection, since if the size of interconnection is increased up to 150μm, the number of the seeded cells in the scaffolds will be decreased. The pore size also clearly affected cell proliferation. It is found that larger pore size is beneficial for cell growth, since more medium exchange can be obtained in larger space. In contrast, the interconnections do not affect cell growth much, since the volume of medium available to the cells is mainly determined by pore size, and not much affected by the pore interconnections.

Vascularization is critical for bone regeneration. Many studies have shown that porosity and pore shape affect the bone in-growth. However, investigation on the effect of pore size and interconnections on vascularization is very limited. A recent study showed that porous structure including interconnection of porous bioceramics affected vascularization, but no quantitative conclusion can be made, since the pore size and interconnection of studied samples were not accurately controlled[13]. In the present study, we evaluated vascularization in a rabbit model using macroporous bioceramic scaffolds with accurately controlled pore size and interconnections, and the results showed that these pore parameters not only affect the size of the blood vessels grown into the porous structure, but also the number of blood vessels formed in the pores of the ceramics. The increase of the pore size only resulted in an increase of the size of the blood vessels growed into the macroporous of the bioceramic scaffolds. However, with the increase of the size of interconnection, both the size and number of the blood vessel formed in the macroporous increased. This phenomenon is understandable, since although the macropores mainly provide the room for the

growth of the blood vessel, but the interconnections are functioning as the door for the in-growth of the blood vessel, so that their size determine the size and number of the blood vessel which allowed to grow into the maropores. So we concluded that the size of interconnections is more important for the vascularization of scaffolds compared with pore size.

An important consideration in the interpretation of current study is that we only used porous scaffolds with round shaped pore structure and interconnections. It is possible that the shape of the pores and interconnections may also affect the cell growth and vascularization. This investigation demonstrated the role of the porous structures such as the diameter of the pores and, in particular, the diameter of the interconnections in cell seeding, cell growth and vascularization, and indicated the importance of these pore parameters in the design of the porous scaffolds for tissue engineering applications. However, optimal pore parameters may be different for different tissue engineering applications, which need to be considered in the design of the scaffolds.

METHODS

Fabrication of β-TCP scaffolds with different microstructure. Porous beta-tricalcium phosphate scaffolds were fabricated by the impregnation of a custom-made organic edifice with β-TCP suspension followed by sintering at 1100℃. All the scaffolds are cylinder in shape with the same dimension of 14mm in diameter and 4mm in height (**Fig.1**). The first set of scaffolds possessed the same interconnection of 120μm and the macropores varied from 300μm to 700μm, the second series of scaffolds had the same macropore of 300-400μm but different interconnections from 70μm to 200μm. The β-TCP disks were sterilized with ethylene oxide and sealed in sterile package until use.

Porosity of β-TCP scaffolds with different microstructure. Each kind of scaffold had a constant porosity. The microstructural characteristics of the different scaffolds were presented in **Table 1**. The density ρ_{sample} of the scaffolds was determined from the mass (m_{sample}, g) and three-dimensional volume (v_{sample}, cm^3) of the fabricated bodies. The porosity P was then calculated by the following equation[22]:

$P = 1-\rho_{sample}/\rho_{solid} = 1- \rho_{relative}$

Where ρ_{solid}=3.07 $g \cdot cm^{-3}$ is the theoretical density of solid β-$Ca_3 (PO4)_2$.[23]

Cell culture. Ten milliliter bone marrows were harvested by aspiration of iliac crest from healthy donor by the same surgeon following written consent from the local Ethics Committee. Each milliliter of bone marrow was inoculated into 100mm culture dish containing α-minimal essential medium (α-MEM) supplemented with 10% selected fetal bovine serum (Gibco, USA), 100IU ml^{-1} penicillin and 100μg ml^{-1}streptomycin (Hyclone, USA) and cultured at 37℃ in a saturated humid CO_2 incubator. The medium was first changed 24 hours after inoculation to remove the unattached cells, and then twice every week until confluence. The attached cells left were mainly human mesenchymal stem cells (hMSCs). The cells were detached with

0.25% trypsin-EDTA and passaged at a density of 10,000 per square centimeter. The second passage of hMSCs were harvested and cryopreserved in the liquid nitrogen until use. The third generation of hMSCs was used for seeding the β-TCP scaffolds.

Cell/β-TCP scaffold composite preparation. The second passage of cryopreserved hMSCs were thawed and cultured in complete α-MEM. When reaching confluence, the third passage of hMSCs were detached and resuspended at 2 million cells per milliliter. The density (D, about 1015.596mg ml^{-1}) of the cell suspension was calculated by dividing the mass with the volume. The mass (M1, mg) of each scaffold was weighed on an electronic balance (Mettler Toledo AB204-E, Switzerland), and then the scaffold was immersed in cell suspension. Vacuum (about 1.9×104 Pa) was generated by a pump to facilitate the penetration of cell suspension into the scaffold. The hybrid composite was put into 100mm culture dish and incubated for 2 hours to ensure attachment of hMSCs. Whereafter, the mass (M2, mg) of each composite was weighed. The difference of M2 and corresponding M1 was the net mass of cell suspension impregnated into the scaffold. Thus, the number (N) of cells seeded into the individual scaffold could be calculated by the following equation: N=(M2-M1)/D×2×106. Then the composite was placed into 12-well plate for culture, followed by addition of 3ml complete α-MEM into each well. The medium was changed completely every 24 hours. For each different microstructural group, the cell/β-TCP composite was cultured for 4 hours, 1, 7 or 14days (n=4 per time point).

Cell viability. Cell viability in the scaffolds was determined by MTT colorimetric method[24-25]. The MTT assay quantitates the ability of mitochondrial dehydrogenases to metabolize the yellow 3-(4, 5-dimethylthiazol-2-yl)-2, 5-diphenyl-tetrazolium bromide to purple formazan which is directly proportional to the number of living cells. In brief, two fifth of the composite was cut off, washed with PBS and transferred into 12-well plate. Then it was cut into small fragments of $3×3×3mm^3$. 1ml of MTT (Sigma, USA) working solution (0.5mg ml^{-1} in PBS) was added into each well. After incubation at 37℃ for 3 hours, the working solution was removed and the samples were grinded into powder. Then the converted dye was solubilized with 2ml acidic isopropanol (0.04 M HCl in absolute isopropanol) by pipetting up and down several times to make sure the converted dye dissolves completely. The dye solution was transferred into a 1.5 ml eppendorf tube and centrifuged at 13,000 rpm for 5 minutes to remove the β-TCP powders. Then the absorbance (A1) of the supernatant was measured on the spectrophotometer at a wavelength of 570nm with background subtraction at 650nm. All the powder of each sample was dried overnight at 60℃ and weighed (M3, mg). The cell viability was expressed as the absorbance (A2=A1*M1/M3) of the whole scaffold.

Histological observation and histomorphometry. As mentioned by Youzhuan, X. et.al[26], half of the scaffolds were fixed in 70% ethanol for 7 days. Then they were dehydrated through graded alcohols (80%~100%), cleared by toluene and embedded in methylmethacrylate without decalcification. The well-polymerized blocks were

shaped in order to cut the sections through the longitudinal axis of the discal scaffold. The sections about 200μm thick were achieved with Leitz SP 1600 (Wetzlar, Germany). Then they were grounded and polished to about 50μm thick with Exakt Grinder (Norderstedt, Germany). All the sections were colored with May-Grünwald Giemsa stain. Two sections from the scaffold center were examined under light microscopy. The cellular adhesion and proliferation inside the scaffold were observed. For the sections from the control group (4 hours after the cell loading), the cell number was counted under every microscopic field (magnification × 100). Each section was divided into 3 equal parts along its longitudinal axis: upper, intermediate and bottom part. For each part 12 fields were evaluated. Then the seeding efficiency and homogeneity among the parts were determined. For those samples after culture, the cell area was quantitatively measured with the aid of semi-automatic software Histolab (Microvision Instruments, Evry, France). The percentage of the cell area /pore area was determined.

In order to estimate the vascularization of the implanted bioceramic scaffolds, the harvested specimens were fixed in 4% paraformaldehyde in PBS for 24h after bisected from tangential to the sagittal suture. The specimens were decalcified in 15% EDTA for 3 weeks at 4 ^{o}C. After dehydrated in gradient series of ethanol (70% ~100%) and cleared in toluene, the samples were embedded in paraffin, 4μm thick sections were cut for hematoxylin–eosin (H&E) staining. Five sequential sections of the central part at each sample were used for histomorphometric analysis. Images of the sections were taken with a Leica MTLA microscope connected with a CCD camera using the same light intensity and exposure. The mean blood vessels size and number were obtained by selected respectively six histological images of the central area and periph area of every paraffin section at 10× magnification in random. For each blood vessel section, only the minor axis was regarded as the size of vessels. All parameters were measured quantitatively using Image pro plus6.0 analysis software.

Surgical model. The animal study was approved by the Standing Committee on Ethics and performed at the Laboratory for Animal Research of the Clinical Research Institute in XiJing hospital of Fourth Military Medical University in China. Ninety six New Zealand white rabbits weighing 3 ± 0.5 kilograms were divided into eight groups according to the type of porous implants in random. The perivertebral fascia lumbodorsalis in each rabbit was exposed under sterile conditions. The rabbits were operated under anesthesia by intravenous injection of 0.5 mg kg^{-1} of Acepromazine Calmivet-Vetoquinol and 10 mg kg^{-1} of Ketamine. The length of incision in the skin of rabbit was about 3 centimeter. Then, the fascia superficialis were separated carefully using the knife holder and the fascia lumbodorsalis abounding in blood vessels were revealed. Two pockets in bilateral perivertebral fascia lumbodorsalis of each rabbit were made according to the size of transplants, and two porous β-TCP blocks with same structure were implanted into the bilateral pockets, then the opening of pockets were sutured. After sufficient irrigation with normal saline, the wound was closed layer by layer.

After operation, the rabbits were prevented from infection by intramuscular

antibiotics injection two times in three days and covering the wound with aseptic dressing. On weeks 1, 2, 4, and 8 after the operation, the rabbits were sacrificed by intravenous injection of an overdose of air, and the implanted β-TCP blocks were collected and fixed in 10% formaldehyde (pH 7.2) for one week.

Statistical analysis. The results were expressed as mean ± standard deviation. Data were analyzed by one-way ANOVA. The $p<0.05$ was considered as statistical significance.

ACKNOWLEDEMENT

This work is supported by the National Basic Science Research Program of China (973 Program) (Grant 2005CB522704) and the Natural Science Foundation of China (Grant 30730034).

AUTHOR CONTRIBUTIONS

Jianxi Lu and Kerong Dai conceived and designed experiments. Kaili Lin, Lei Chen and Jianxi Lu fabricated β-TCP scaffolds with different microstructure. Feng Bai and Xiaojiang Sun performed cell and animal experiments. All data analyses were performed by Feng Bai , Xiaojiang Sun, Zheng Wang, Jiang Chang, Kerong Dai and Jianxi Lu. The manuscript was written by Jiang Chang, Zheng Wang and Feng Bai.

1. Vassilis, K.& David, K. Porosity of 3D biomaterial scaffolds and osteogenesis. *Biomaterials* **26**,5474–5491（2005）.
2. Debi, P. *et al*. Effect of 3D-microstructure of bioabsorbable PGA: TMC scaffolds on the growth of chondrogenic cells. *J Biomed Mater Res B*.**88**, 92-102(2009).
3. Zeltinger, J., Sherwood, J.K., Graham, D.A., Mueller, R.& Griffith, L.G. Effect of pore size and void fraction on cellular adhesion, proliferation, and matrix deposition. *Tissue Eng.* 7, 557–572(2001).
4. Kruyt, M.C. *et al*. Viable osteogenic cells are obligatory for tissue-engineered ectopic bone formation in goats. *Tissue Eng.* **9**, 327–336(2003).
5. Min, L., Benjamin, M. & James, C. Y. Effect of scaffold architecture and pore size on smooth muscle cell growth. *J Biomed Mater Res A*. **87**, 1010-1016(2009).
6. Roy, T.D. *et al*. Performance of degradable composite bone repair products made via three-dimensional fabrication techniques. *J Biomed Mater Res A*. **66**, 283–291(2003).
7. Jonathan, I. *et al*. Development of specific collagen scaffolds to support the osteogenic and chondrogenic differentiation of human bone marrow stromal cells. *Biomaterials* **29**,3105–3116(2008).
8. Flautre, B., Descamps, M., Delecourt, C., Blary, M. & Hardouin, P. Porous HA ceramic for bone replacement: role of the pores and interconnections-experimental study in the rabbit. *J. Mater. Sci. Mater. Med.* **12**, 679–682(2001).
9. Gauthier, O., Bouler, J.M., Aguado, E., Pilet, P. & Daculsi, G. Macroporous biphasic calcium phosphate ceramics: influence of macropore diameter and macroporosity percentage on bone ingrowth. *Biomaterials* **19**, 133–139(1998).
10. Kuboki, Y., Jin, Q. & Takita, H. Geometry of carriers controlling phenotypic expression in BMP-induced osteogenesis and chondrogenesis. *J Bone Joint Surg Am.* **83**,

105–115(2001).
11. Kuboki, Y., Jin, Q., & Kikuchi, M., Mamood, J. & Takita, H. Geometry of artificial ECM: sizes of pores controlling phenotype expression in BMP-induced osteogenesis and chondrogenesis. *Connect Tissue Res*. **43**, 529–34(2002).
12. Mikos, A.G. *et al*. Prevascularization of porous biodegradable polymer. *Biotechnol Bioeng*. **42**,716–723(1993).
13. Lu, J. *et al.*Role of interconnections in porous bioceramics on bone recolonization in vitro and in vivo. *J. Mater. Sci. Mater. Med.* **10**,111–120(1999).
14. Mitsuru, T. *et al.* Mechanical properties and osteoconductivity of porous bioactive titanium. *Biomaterials* **26**, 6014–6023(2005).
15. Angela, S.P., Thomas, H.B., Sarah, H.C. & Robert, E.G. Microarchitectural and mechanical characterization of oriented porous polymer scaffolds. *Biomaterials* **24**,481–489(2003).
16. Charriere, E., Lemaitre,J. & Zysset, P. Hydroxyapatite cement scaffolds with controlled macroporosity: fabrication protocol and mechanical properties. *Biomaterials* **24**, 809–817(2003).
17. Agrawal, C. & Ray, R. Biodegradable polymeric scaffolds for musculoskeletal tissue engineering. *J Biomed Mater Res* . **55**,141–150(2001).
18. Jin, Q.M. *et al*. Effects of geometry of hydroxyapatite as a cell substratum in BMP-induced ectopic bone formation. *J Biomed Mater Res*. **51**,491–499(2000)
19. Hulbert, S.F. *et al*. Potential of ceramic materials as permanently implantable skeletal prostheses. *J Biomed Mater Res* .**4**, 433–56(1970).
20. Tsuruga, E., Takita, H., Itoh, H., Wakisaka, Y. & Kuboki, Y. Pore size of porous hydroxyapatite as the cell-substratum controls BMP induced osteogenesis. *J Biochem (Tokyo)*.**121**, 317–324 (1997).
21. Descamps, M. *et al*. Manufacture of macroporous β-tricalcium phosphate bioceramics. *Journal of the European Ceramic Society*. **28**, 149–157(2008).
22. Qizhi, Z., Chenlan, D., Thompson, Aldo, R. & Boccaccini. 45S5 Bioglasss-derived glass-ceramic scaffolds for bone tissue engineering, *Biomaterials* **27**, 2414-2425(2006).
23. Larry, L. & Hench. Bioceramics**.** *J. Am. Ceram. Soc.* **81**, 1705–1728 (1998).
24. Xiaoming, O., Kevin, C., Jean, C. & Shi, H. Monoamine oxidase A and repressor R1 are involved in apoptotic signaling pathway. *PNAS*.**103**, 10923–10928(2006).
25. Xia, L. *et al*. Sumoylation of nucleophosmin/B23 regulatesits subcellular localization, mediating cell proliferation and survival. *PNAS*. 104, 9679–9684(2007).
26. Youzhuan, X. *et al*. Three-dimensional flow perfusion culture system for stem cell proliferation inside the critical – size β-tricalcium phosphate scaffold. *Tissue Engineering* **12**, 3535-3543(2006).

Figure 1 Process of macroporous bioceramics. A. Plastic microspheres. B. Assembly of microspheres as macroporous templates. C. Bioceramic powders. D. Bioceramic slurry. E. Casting of bioceramic slurry into the templates. F. Sintered macroporous bioceramic block. E. SEM micrograph of macroporous bioceramic block. H. Interconnection of the macroporoes.

Figure 2 Scanning electron micrographs of the ceramic scaffolds with different size of pores and interconnections. (**a-d**) The scaffolds with constant interconnection of 120μm and different macropores size (**a**.300-400μm, **b**.400-500μm, **c**.500-600μm and **d**.600-700μm).(**e-h**) The scaffolds with constant macropore of 300-400μm and different interconnections size(**e**.70μm, **f.**100μm, **g**.120μm, **h**.150μm). Bar =100μm.

Figure 3 Compressive strength and porosities of the ceramic scaffolds with different size of pores and interconnections. (**a,b**)Scaffolds with same size of interconnection (120μm) showed decreased porosity and increased compressive strength with increased pore size. (**c,d**)Scaffolds with same pore size (300-400μm) showed increased porosity and decreased compressive strength with increased size of interconnection (from 70 to 120μm). (**e,f**) Scaffolds with same pore size (500-600μm) showed increased porosity and decreased compressive strength with increased size of interconnection (from 120 to 200μm).

Figure 4 Effect of pore size and interconnections on cell seedings. (**a**) The number of cells seeded into the scaffold with the same interconnection (120μm) but different size of macropores. When the interconnection is fixed in 120μm , the number of seeded cells in scaffolds with pore size of 300-400μm is higher than the scaffolds with pore size between 400-700μm ($*p<0.01$). (**b**) The number of cells seeded into the scaffold with constant macropore (300-400μm) but different interconnections. In the scaffolds with constant size of macropores (300-400μm) and different interconnections the number of seeded cells in the scaffolds with an interconnection of 150μm is the lowest as compared with other samples ($*p<0.01$). (Error bars indicate SD; n=6)

Figure 5 Cell proliferation in macroporous scaffolds with different macropores and interconnections. (**a**) The scaffolds with constant interconnection of 120μm and a macropore size of 500-600μm showed the highest cell proliferation; (**b**) No difference in cell proliferation in the scaffolds with constant macropore size of 300-400μm and different interconnection. (Error bars indicate SD; n=4)

Figure 6 Effect of interconnections on the size and number of the blood vessels. (**a-d**)Light microscopic findings in four kinds of scaffolds with different interconnection size (**a.** 70μm, **b.**100μm, **c.**150μm and **d.**200μm) and the constant pore size (300-400μm) four weeks after implantation. The blood vessels tended to be more dense and have larger size in the scaffolds with larger interconnection (**c.**150μm and **d.**200μm) than in those with smaller interconnection(**a.** 70μm and **b.**100μm). Bar=100μm. TCP=β-tricalcium phosphate; FT=fibrous tissue; RBC= red blood cells.

Red arrow indicates blood vessel. (**e**) The size of blood vessels in macroporous scaffolds with constant pore size (300-400μm) and different interconnections. Increase of the interconnection resulted in an increase of the size of the blood vessel. (**f**)The number of blood vessels in macroporous scaffolds with constant pore size (300-400μm) and different interconnections. Increase of the interconnection resulted in an increase of the number of the blood vessels. (Error bars indicate SD; n=6)

Figure 7 Effect of macropores on the size and number of the blood vessels. (**a-d**)Light microscopic findings in four kinds of scaffolds with different pore size (**a.** 300-400μm, **b.**400-500μm, **c.**500-600μm and **d.**600-700μm) and the constant interconnection size (120μm) four weeks after implantation. The larger blood vessels were found in the scaffolds with larger pore size (**b.**400-500μm, **c.**500-600μm and **d.**600-700μm). Bar=100μm. TCP=β-tricalcium phosphate; FT=fibrous tissue. Red arrow indicates blood vessel. (**e**) The size of blood vessels in macroporous scaffolds with constant interconnection (120μm) and different pore size. Large pore size is beneficial for the growth of blood vessels, and the pore size smaller than 400μm limits the growth of blood vessels and resulted in a smaller blood vessel diameter. Blood vessels grow fast within the porous scaffolds in the first 2 weeks, and then become stabilized, suggesting that the first 2 weeks are critical for development of the size of the blood vessels. (**f**) The number of blood vessels in macroporous scaffolds with constant interconnection (120μm) and different pore size. No significant difference in the number of the blood vessels was observed between the samples with different pore size. It is noticed that the number of blood vessels increased within the first 4 weeks in all samples and then become stabilized, suggesting that the number of the blood vessels was determined in the first 4 weeks after implantation. (Error bars indicate SD; n=6)

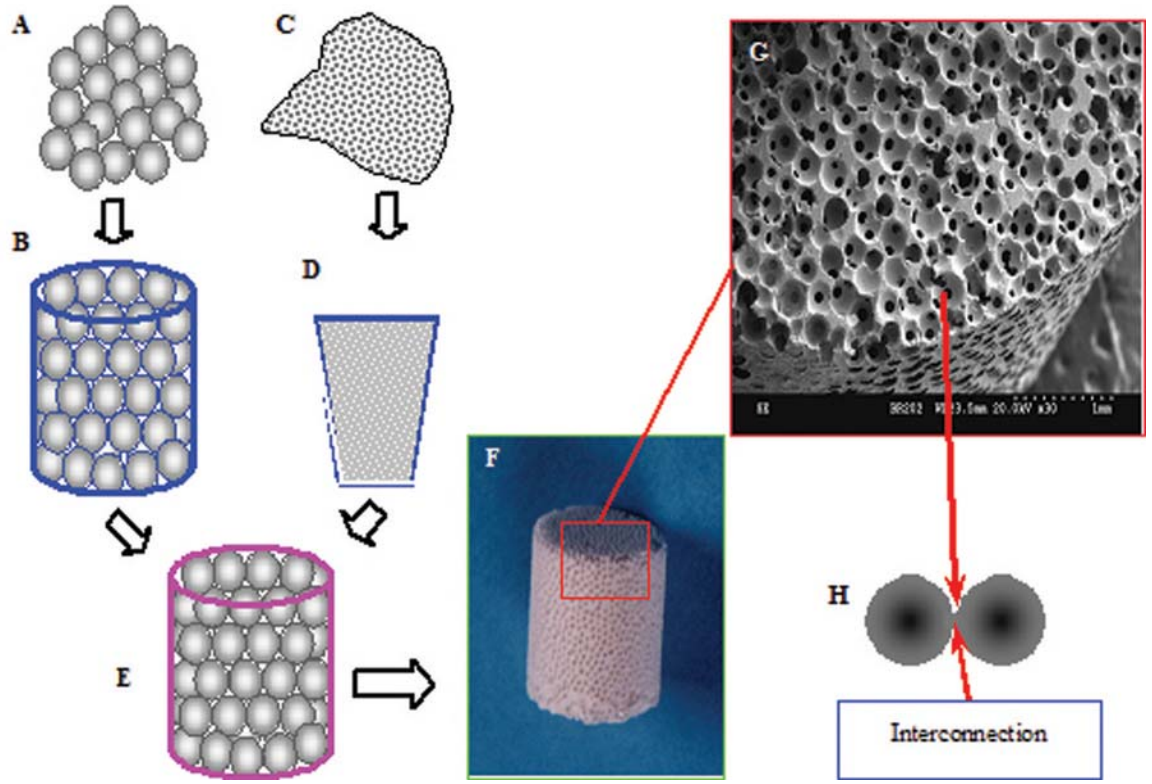
A
C
B
D
E
F
G
H
Interconnection

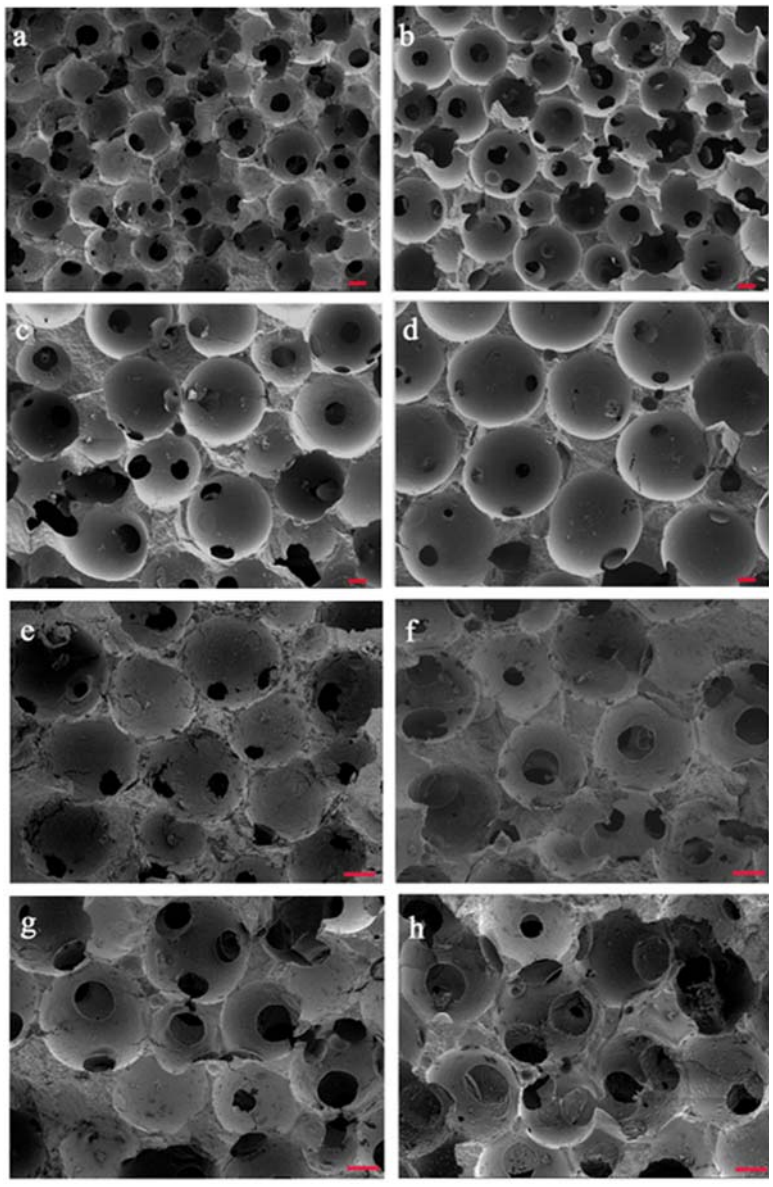
a
b
c
d
e
f
g
h

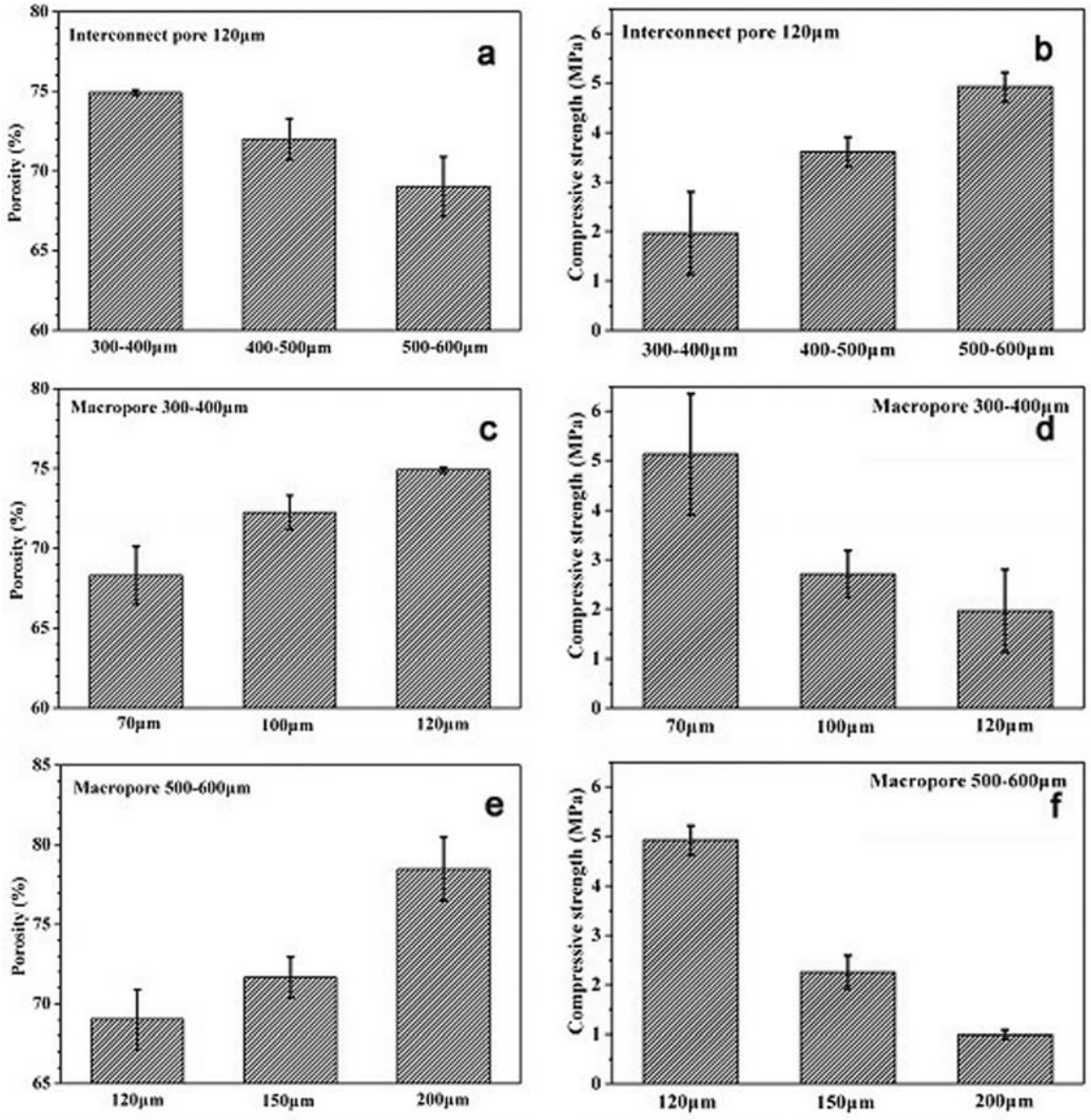
Interconnect pore 120μm
a
Porosity (%)
80
75
70
65
60
300-400μm
400-500μm
500-600μm
Interconnect pore 120μm
b
Compressive strength (MPa)
6
5
4
3
2
1
0
300-400μm
400-500μm
500-600μm
Macropore 300-400μm
c
Porosity (%)
80
75
70
65
60
70μm
100μm
120μm
Macropore 300-400μm
d
Compressive strength (MPa)
6
5
4
3
2
1
0
70μm
100μm
120μm
Macropore 500-600μm
e
Porosity (%)
85
80
75
70
65
120μm
150μm
200μm
Macropore 500-600μm
f
Compressive strength (MPa)
6
5
4
3
2
1
0
120μm
150μm
200μm

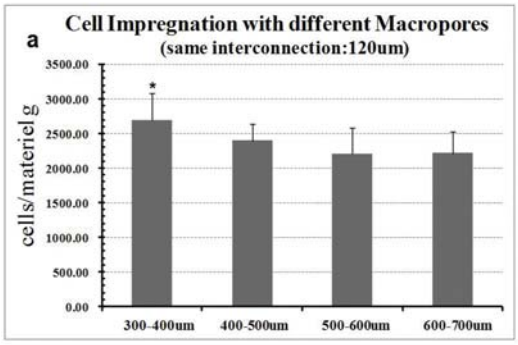
a
Cell Impregnation with different Macropores
(same interconnection:120um)
cells/materiel g
3500.00
3000.00
2500.00
2000.00
1500.00
1000.00
500.00
0.00
*
300-400um
400-500um
500-600um
600-700um

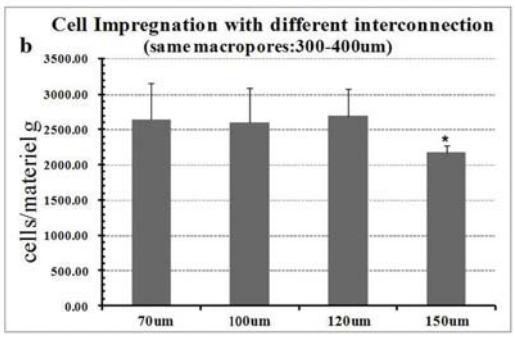
b
Cell Impregnation with different interconnection
(same macropores:300-400um)
cells/materiel g
3500.00
3000.00
2500.00
2000.00
1500.00
1000.00
500.00
0.00
*
70um
100um
120um
150um

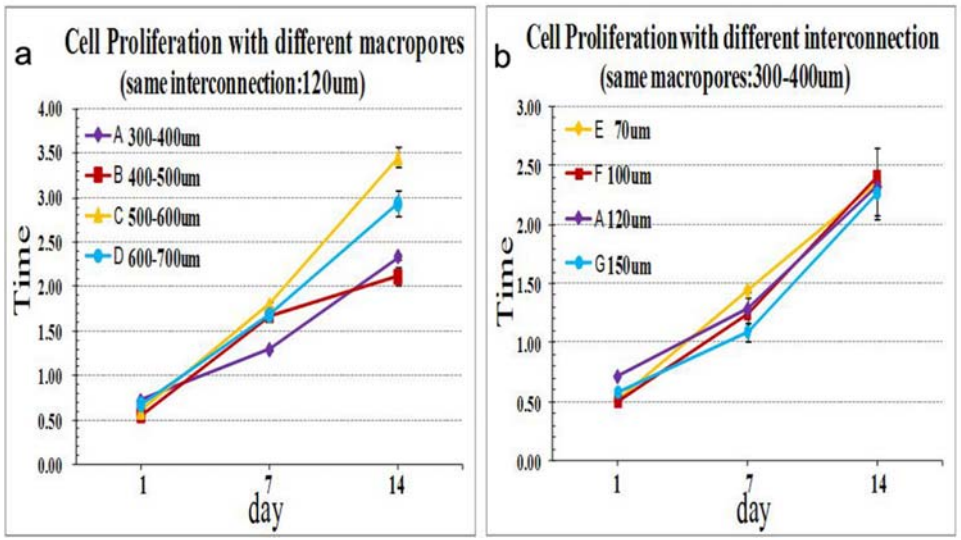
a
Cell Proliferation with different macropores
(same interconnection:120um)
A 300-400um
B 400-500um
C 500-600um
D 600-700um
Time
day
b
Cell Proliferation with different interconnection
(same macropores:300-400um)
E 70um
F 100um
A 120um
G 150um
Time
day

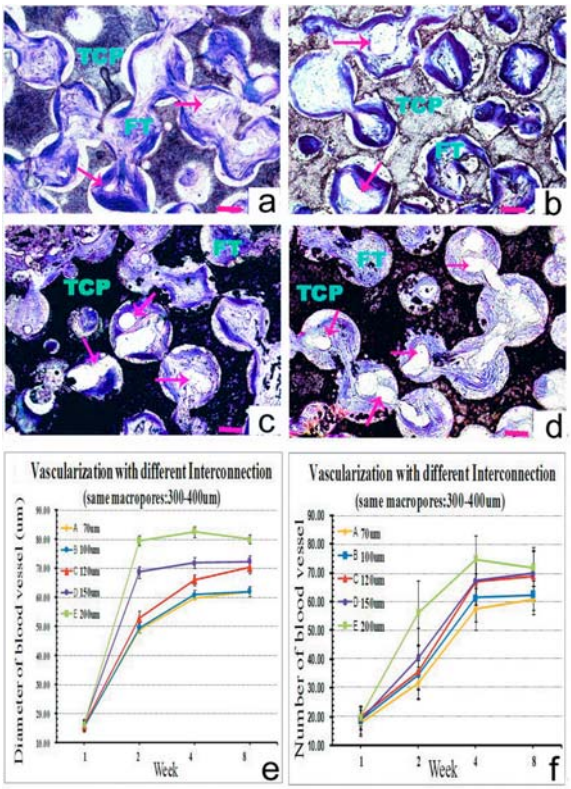
TCP
FT
a
TCP
FT
b
FT
TCP
c
FT
TCP
d
Vascularization with different Interconnection
(same macropores:300-400um)
Diameter of blood vessel (um)
A 70um
B 100um
C 120um
D 150um
E 200um
Week
e
Vascularization with different Interconnection
(same macropores:300-400um)
Number of blood vessel
A 70um
B 100um
C 120um
D 150um
E 200um
Week
f

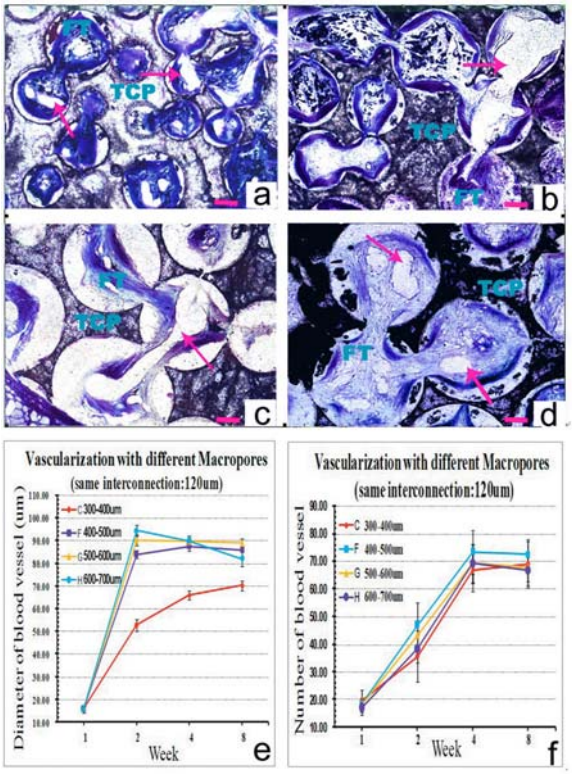
FT
TCP
a
TCP
FT
b
FT
TCP
c
TCP
FT
d
Vascularization with different Macropores
(same interconnection:120um)
Diameter of blood vessel (um)
C 300-400um
F 400-500um
G 500-600um
H 600-700um
Week
e
Vascularization with different Macropores
(same interconnection:120um)
Number of blood vessel
C 300-400um
F 400-500um
G 500-600um
H 600-700um
Week
f

Table 1. The theoretical and measured pore size and the size of interconnections

No	Theoretical Pore size (μm)	Theoretical Interconnections (μm)	The measured Pores size (μm)	The measured Interconnections (μm)	Porosity%
A	**300-400**	**70**	**330.5±26.6**	**72.35±3.39**	**68.30±1.82**
B	**300-400**	**100**	**321.6±12.5**	**104.53±12.69**	**72.76±1.07**
C	**300-400**	**120**	**316.2±22.7**	**118.11±13.82**	**74.90±1.60**
D	**300-400**	**150**	**321.3±34.5**	**149.69±12.51**	**77.87±2.41**
E	**300-400**	**200**	**315.7±28.1**	**198.31±10.20**	**79.39±1.68**
F	**400-500**	**120**	**402.3±25.6**	**117.64±12.60**	**72.02±1.29**
G	**500-600**	**120**	**524.7±36.8**	**121.66±13.85**	**69.03±1.87**
H	**600-700**	**120**	**621.1±32.2**	**118.35±13.66**	**67.01±2.23**